Closed-Loop Asynchronous Neuromuscular Electrical Stimulation Prolongs Functional Movements in the Lower Body

Ryan J. Downey, Teng-Hu Cheng, Matthew J. Bellman, and Warren E. Dixon

***Abstract*—Neuromuscular electrical stimulation (NMES) is commonly used in rehabilitative settings and is also used for assistive purposes to create functional movements, where it is termed functional electrical stimulation (FES). One limitation of NMES/FES is early onset of muscle fatigue. NMES-induced fatigue can be reduced by switching between multiple stimulation channels that target different motor units or synergistic muscles (i.e., asynchronous stimulation). However, switching stimulation channels introduces additional complexity due to the need to consider the switching dynamics and differing muscle response to stimulation. The objective of this study was to develop and test a closed-loop controller for asynchronous stimulation. The developed closed-loop controller yields asymptotic tracking of a desired trajectory for a person's knee-shank complex despite switching between stimulation channels. The developed controller was implemented on four able-bodied individuals with four-channel asynchronous stimulation as well as single-channel conventional stimulation. The results indicate that asynchronous stimulation extends the duration that functional movements can be performed during feedback control. This result is promising for the implementation of asynchronous stimulation in closed-loop rehabilitative procedures and in assistive devices as a method to reduce muscle fatigue while maintaining a person's ability to track a desired limb trajectory.**

***Index Terms*—Asynchronous stimulation, closed-loop control, fatigue, functional electrical stimulation (FES), neuromuscular electrical stimulation (NMES).**

I. Introduction

NEUROMUSCULAR electrical stimulation (NMES) is commonly used for rehabilitation and has been shown to impart a number of health benefits [1]–[5]. However, the early onset of muscle fatigue limits the duration that NMES can be applied, thereby limiting the imparted health benefits. Furthermore, NMES can be used to evoke functional outcomes [6], [7], where it is termed functional electrical stimulation (FES). However, NMES-induced fatigue limits the duration that functional tasks can be performed. Therefore, researchers have examined methods to slow the rate of fatigue [8]–[12].

One suggested cause of fatigue is that, in contrast to the Henneman size principle for voluntary motor unit recruitment [13], large, quick fatiguing motor units are preferentially recruited over slow fatiguing motor units during NMES. While a reversal of the size principal has been commonly suggested [14], [15], some research contends that NMES-induced motor unit recruitment is nonselective without preference to muscle fiber type [16], [17]. Another commonly suggested cause of fatigue is that, in contrast to volitional contractions, motor units are activated synchronously during NMES [16], [17]. Ultimately, higher stimulation frequencies are required to achieve a smooth force output (i.e., fused tetanus) when recruited muscle fibers are activated synchronously rather than asynchronously due to the temporal summation of the muscle force output. Since high stimulation frequencies are associated with the early onset of fatigue [18]–[20], low stimulation frequencies should be utilized to minimize fatigue or sustain a desired functional outcome. Researchers have developed two similar stimulation methods to counteract this suggested cause of fatigue: sequential stimulation and asynchronous stimulation.

During sequential stimulation, multiple stimulation channels are utilized to either segregate the desired muscle into multiple groups of motor units or to segregate multiple synergistic muscles. Pulse trains are then delivered sequentially to each stimulation channel, thereby allowing motor units to rest when the corresponding stimulation channel is not active. Lower rates of fatigue can be attributed to a reduced duty cycle (i.e., a lower average stimulation frequency) for the recruited motor units compared to conventional single-channel stimulation. Similar to sequential stimulation, asynchronous stimulation utilizes multiple stimulation channels to segregate motor units or synergistic muscles. However, during asynchronous stimulation, the stimulus pulses are delivered in an interleaved manner so that low stimulation frequencies are achieved at each stimulation channel while retaining a high composite stimulation frequency. Lower rates of fatigue during asynchronous stimulation can similarly be attributed to a reduced stimulation frequency of the recruited motor units. An illustrative comparison of sequential, asynchronous, and conventional stimulation is provided in Fig. 1.

Both asynchronous stimulation [21]–[34] and sequential stimulation [35]–[38] have been shown to reduce NMES-induced fatigue; however, previous studies have primarily

Manuscript received November 03, 2014; revised March 13, 2015; accepted April 17, 2015. Date of publication April 29, 2015; date of current version November 04, 2015. This research is supported in part by the National Science Foundation under Award 1161260. Any opinions, findings and conclusions or recommendations expressed in this material are those of the author(s) and do not necessarily reflect the views of the sponsoring agency.

The authors are with the Department of Mechanical and Aerospace Engineering, University of Florida, Gainesville FL 32611 USA (e-mail: ryan2318@ufl.edu; tenghu@ufl.edu; mattjo@ufl.edu; wdixon@ufl.edu).

Color versions of one or more of the figures in this paper are available online at http://ieeexplore.ieee.org.

Digital Object Identifier 10.1109/TNSRE.2015.2427658

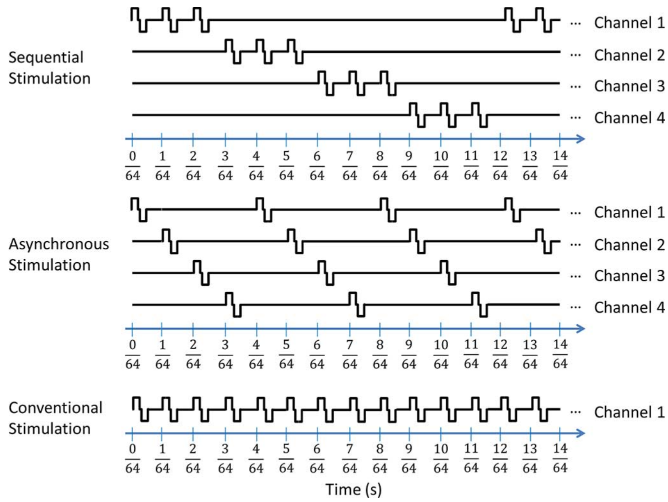

Fig. 1. During sequential stimulation, high frequency pulse trains are delivered sequentially to multiple channels, resulting in a lower average stimulation frequency per channel. In the present example, each stimulation channel receives pulses at 64 Hz; however, the average stimulation frequency is 16 Hz per channel. During asynchronous stimulation, multiple channels are utilized where high composite stimulation frequencies are achieved by interleaving the pulses. Depicted is asynchronous 16 Hz stimulation with four channels where each channel receives pulse trains at 16 Hz, but the composite stimulation frequency is 64 Hz. During conventional stimulation, only a single stimulation channel is utilized, and higher stimulation frequencies are required to achieve a strong and smooth force output, resulting in the onset of fatigue. Depicted in the present example is 64 Hz conventional stimulation. The pulsewidths are not drawn to scale for illustrative purposes.

focused on isometric contractions with fixed stimulation parameters (i.e., open-loop stimulation) [21]–[25], [28]–[32], [34], [36], [37]. Therefore, it is presently unclear if the fatigue benefits reported for open-loop stimulation similarly applies to feedback control of NMES in man. One study [36] found that a shorter on-time (i.e., the time to keep one stimulation channel activated before switching to the next channel) resulted in less fatigue, motivating the use of asynchronous stimulation over sequential stimulation. However, incorporating either of these stimulation strategies with a closed-loop controller is challenging due to the need to switch between different synergistic muscles (or different groups of motor units within a given muscle) while maintaining stability of the closed-loop system. Specifically, the muscle's response to a given stimulus will differ for each stimulation channel since each channel activates a different number and/or type of motor units. Thus, there is a need to design a controller that considers the switching dynamics and muscle response to stimulation. Since both stimulation methods exhibit the same closed-loop control challenges and asynchronous stimulation is more commonly used, the subsequent limb model and control development sections will refer only to asynchronous stimulation without loss of generality.

Based on the preliminary work in [39], a closed-loop tracking controller is developed for asynchronous stimulation. The associated stability analysis yields semi-global asymptotic tracking despite switching between stimulation channels, parametric uncertainties in the nonlinear dynamics, and the presence of exogenous disturbances. As a result of the designed transition period, which can be made arbitrarily short by adjusting the control gains, switching is arbitrary in the sense that the switching signal is not dependent on the states and the switching can be arbitrarily fast. The developed controller is applied to both asynchronous and conventional stimulation in experiments with a modified leg extension machine to compare the ability of each stimulation method to maintain trajectory tracking. Asynchronous stimulation with the developed closed-loop controller is found to significantly prolong the functional movements of the lower limb. This result is promising for the implementation of asynchronous stimulation in closed-loop rehabilitative procedures and in assistive devices as a method to reduce fatigue while maintaining a person's ability to track a desired limb trajectory.

II. Limb Model

The knee-joint dynamics are modeled as in [40] as

$$M_I + M_e + M_g + M_v + \tau_d = \tau \tag{1}$$

where $M_I : \mathbb{R} \to \mathbb{R}$ denotes the inertial effects of the shank-foot complex about the knee-joint; $M_e : \mathbb{R} \to \mathbb{R}$ denotes the elastic effects due to joint stiffness; $M_g : \mathbb{R} \to \mathbb{R}$ denotes the gravitational effects on the limb; $M_v : \mathbb{R} \to \mathbb{R}$ denotes the viscous effects due to damping in the musculotendon complex; $\tau_d \in \mathbb{R}$ denotes an unknown time-varying disturbance that is assumed to be sufficiently smooth in the sense that $\tau_d, \dot{\tau}_d, \ddot{\tau}_d \in \mathcal{L}_\infty$; and $\tau \in \mathbb{R}$ denotes the torque produced at the knee-joint due to stimulation. The inertial and gravitational effects in (1) are modeled as

$$M_I \triangleq J\ddot{q}, \quad M_g \triangleq mgl\sin(q) \tag{2}$$

where $J,\ m,\ g,\ l \in \mathbb{R}$ are positive constants, and $q,\ \dot{q},\ \ddot{q} \in \mathbb{R}$ denote the angular position (depicted in Fig. 2), velocity, and acceleration of the shank about the knee-joint, respectively. The terms $J,\ m$, and l denote the unknown inertia of the combined shank and foot, the unknown combined mass of the shank and foot, and the unknown distance between the knee-joint and the lumped center of mass of the shank and foot, respectively, while g denotes the gravitational acceleration constant. The elastic and viscous effects are modeled as in [40] as

$$M_e \triangleq k_{e1} e^{-k_{e2} q}(q - k_{e3})$$

where $k_{e1}, k_{e2}, k_{e3} \in \mathbb{R}$ are unknown constants and

$$M_v \triangleq -B_1 \tanh(-B_2 \dot{q}) + B_3 \dot{q}$$

where $B_1, B_2, B_3 \in \mathbb{R}$ are unknown, positive constants.

Asynchronous stimulation involves switching between $N \in \mathbb{N}$ stimulation channels. Since each channel activates different sets of motor units, the corresponding dynamics are different depending on which stimulation channel is active. Let $\mathbb{S} \subset \mathbb{N}$ be the finite index set for all stimulation channels, defined as

$$\mathbb{S} \triangleq \{1,\ 2,\ 3, \ldots,\ N\}.$$

Then, the torque produced by stimulation of the ith subsystem is related to the musculotendon force as

$$\tau_i \triangleq \varsigma_i F_{T,i}, \quad i \in \mathbb{S} \tag{3}$$

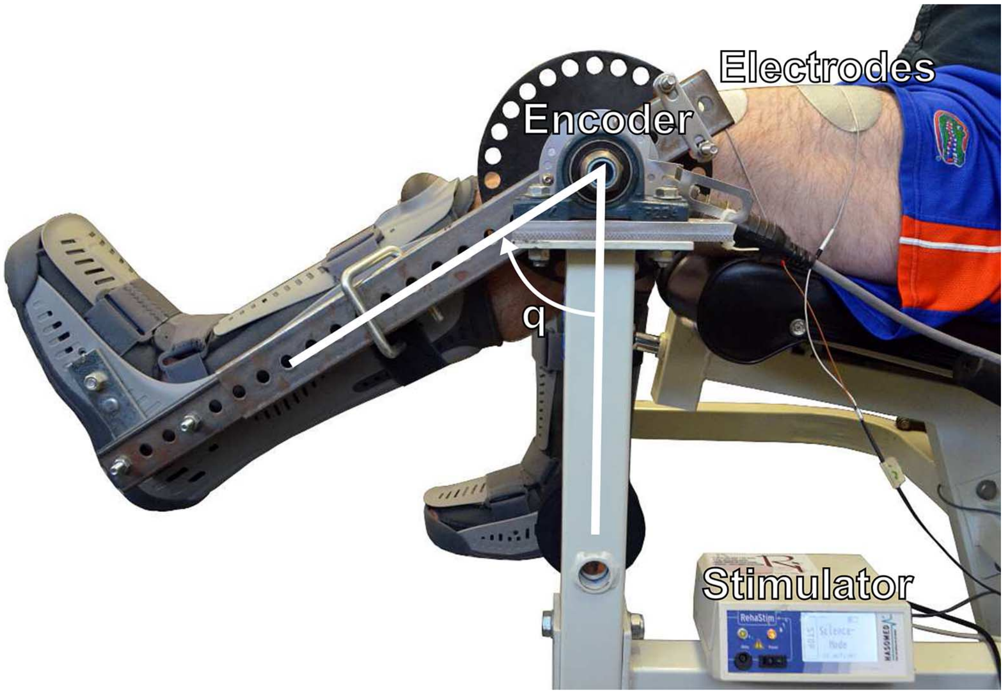

Fig. 2. Modified leg extension machine was fitted with optical encoders to measure the knee joint angle q and provide feedback to the developed control algorithm running on a personal computer. Participants were seated at the leg extension machine with the thighs parallel to the ground and hips flexed approximately 75°. The desired stimulation parameters were sent in real time from a personal computer to the stimulator via USB.

where $\varsigma_i \in \mathbb{R}$ denotes an unknown, positive moment arm that changes with extension and flexion of the leg. The musculotendon force $F_{T,i} \in \mathbb{R}$ is defined as

$$F_{T,i} \triangleq F_i \cos(a_i), \quad i \in \mathbb{S} \tag{4}$$

where $a_i \in \mathbb{R}$ denotes the pennation angle between the tendon and the muscle, which changes with extension and flexion of the leg, and $F_i \in \mathbb{R}$ denotes the force produced by the recruited motor units in the ith subsystem. The relationship between muscle force and applied voltage is defined as

$$F_i \triangleq \varphi_i \eta_i V_i, \quad i \in \mathbb{S} \tag{5}$$

where $V_i \in \mathbb{R}$ represents the voltage applied to the ith subsystem by electrical stimulation; $\eta_i \in \mathbb{R}$ is an unknown function of q and $\dot{q}$ (i.e., η_i represents unknown muscle force-length and force-velocity relationships); and $\varphi_i \in \mathbb{R}$ is an unknown time-varying function that represents fatigue.

Typically, during asynchronous stimulation, only one channel is activated at a given time. However, if only one stimulation channel is activated at a given time, immediately switching the applied voltage from one subsystem to another subsystem would introduce discontinuities in the torque produced at the knee. Therefore, switching in the subsequent development is designed to include an arbitrarily short period of time during which both subsystems are simultaneously activated (each receiving a percentage of the input voltage). During the transition period, the voltage input transitions from being applied solely to the original subsystem to being applied to the new subsystem designated by the switching signal. Without loss of generality, the knee-joint dynamics during stimulation of up to two subsystems at a time can be modeled as

$$M_I + M_e + M_g + M_v + \tau_d = \tau_i + \tau_j \tag{6}$$

where $\tau_i, \tau_j \in \mathbb{R}$ denote the torque produced by stimulation of the ith and jth subsystems, respectively, for $i, j \in \mathbb{S}, i \neq j$. The inertial, gravitational, elastic, and viscous components are common to all subsystems since all subsystems act on the same knee joint, and the unknown, bounded disturbance torque is also common to all subsystems.

Remark 1: Equation (6) implicitly assumes that there is no activation overlap between any of the stimulation channels (i.e., a specific muscle fiber generates tension in response to only one channel), although there is likely to be some overlap. Activation overlap would cause some motor units to be activated more frequently than desired, leading to increased muscle fatigue. Therefore, overlap should be avoided in practice since the motivation for asynchronous stimulation is to reduce fatigue. However, activation overlap would not have a negative effect from a control perspective. For example, 100% activation overlap for all of the channels would imply that there is effectively only one stimulation channel, and thus, the tracking control problem would simplify to single-channel conventional stimulation.

III. Control Development

The control objective is to enable the knee joint to track a specified desired angular trajectory. To quantify this objective, the position tracking error is defined as

$$e_1 \triangleq q_d - q \tag{7}$$

where $q_d \in \mathbb{R}$ denotes the desired angular trajectory for the knee joint, designed such that $q_d, q_d^k \in \mathcal{L}_\infty$, where q_d^k denotes the kth derivative of q_d for $k = 1, 2, 3, 4$. To facilitate the subsequent development, auxiliary tracking errors $e_2, r \in \mathbb{R}$ are defined as

$$e_2 \triangleq \dot{e}_1 + \alpha_1 e_1 \quad (8)$$
$$r \triangleq \dot{e}_2 + \alpha_2 e_2 \quad (9)$$

where $\alpha_1, \alpha_2 \in \mathbb{R}$ are selectable positive constants. The filtered tracking error r facilitates the stability analysis but is not used in the control development due to the dependence on the angular acceleration about the knee, which is assumed to be unmeasurable.

After multiplying (9) by J, and utilizing (2) and (6)–(8), the open-loop dynamics during stimulation of up to two subsystems can be written as

$$Jr = W - \tau_i - \tau_j + \tau_d, \; i, j \in \mathbb{S}, \; i \neq j \quad (10)$$

where $W \in \mathbb{R}$ denotes an auxiliary term defined as

$$W \triangleq J(\ddot{q}_d + \alpha_1 \dot{e}_1 + \alpha_2 e_2) + M_e + M_g + M_v.$$

After utilizing (3)–(5), the open-loop dynamics in (10) can be expressed as

$$Jr = W - V_i \Omega_i - V_j \Omega_j + \tau_d, \; i, j \in \mathbb{S}, \; i \neq j \quad (11)$$

where $V_i \in \mathbb{R}$ denotes the voltage applied by the ith stimulation channel, and $\Omega_i \in \mathbb{R}$ denotes an unknown positive auxiliary function of the leg angle and velocity that varies with time and relates the voltage applied by the ith channel to the torque produced by the activated motor neurons, defined based on [40] as

$$\Omega_i \triangleq \varsigma_i \varphi_i \eta_i \cos(a_i), \; i \in \mathbb{S}. \quad (12)$$

Assumption 1: The moment arm ς_i is assumed to be a nonzero, positive, and bounded function [41] where the first two partial derivatives of ς_i with respect to q exist and are bounded for a bounded argument. Likewise, the function η_i is assumed to be a nonzero, positive, and bounded function [42] provided the muscle is not fully stretched or contracting concentrically at its maximum shortening velocity [43], where the first two partial derivatives of η_i with respect to q and $\dot{q}$ exist and are bounded for a bounded argument. The unknown fatigue function φ_i is assumed to be a nonzero, positive, and bounded function of time with bounded first and second time derivatives. Thus, from (12), the first two partial derivatives of Ω_i with respect to q and $\dot{q}$ are assumed to exist and be bounded for a bounded argument; the first two partial derivatives of Ω_i with respect to time (via the time derivatives of φ_i) are assumed to exist and be bounded; and Ω_i is assumed to be a nonzero, positive, and bounded function such that $\Omega_i > \varepsilon > 0, \; \forall i \in \mathbb{S}$, where $\varepsilon \in \mathbb{R}$ is a known positive constant.

Let $\sigma : [0, \infty) \rightarrow \mathbb{S}$ denote a piecewise constant signal that selects a stimulation channel from $\mathbb{S}$ to be activated at time $t \in [0, \infty)$. The instants when the value of σ changes are called the switching times, t_k. Immediately following each switching time, there is a transition period $\triangle t$ during which the input voltage is transitioned from one channel to another.

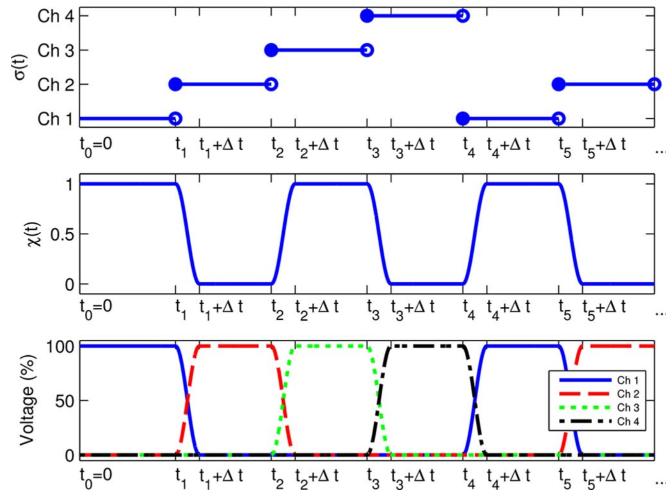

Fig. 3. Depicted is an example piecewise constant switching signal σ that selects a desired stimulation channel to be active. Combining the switching signal with the corresponding signal χ results in a smooth transition of the control voltage between stimulation channels as seen in the bottom subplot.

Property 1: The designed switching signal σ has a finite number of discontinuities on any bounded time interval. Any two consecutive switching times, t_k and t_{k+1} satisfy $t_k + \Delta t < t_{k+1} \forall\, k \in \mathbb{N} \cup \{0\}$, and the switching signal σ remains constant for $t \in [t_k, t_{k+1})$.

Let $V \in \mathbb{R}$ denote the voltage input to the system such that $V \triangleq V_i + V_j$, where

$$V_i \triangleq \chi V, \quad V_j \triangleq (1 - \chi) V \quad (13)$$

where $\chi \in \mathbb{R}$ is an auxiliary signal designed such that $0 \leq \chi \leq 1$ so that the transition from one stimulation channel to another is continuous. Fig. 3 illustrates a particular choice of χ that facilitates the transition between channels based on the switching signal σ, where χ is selected as

$$\chi \triangleq \begin{cases} 1 & t \in [t_0, t_1) \\ \frac{1+\cos(\omega(t-t_k))}{2} & t \in \bigcup\limits_{k \in \mathbb{N}_{\text{odd}}} [t_k, t_k + \Delta t) \\ 0 & t \in \bigcup\limits_{k \in \mathbb{N}_{\text{odd}}} [t_k + \Delta t, t_{k+1}) \\ \frac{1-\cos(\omega(t-t_k))}{2} & t \in \bigcup\limits_{k \in \mathbb{N}_{\text{even}}} [t_k, t_k + \Delta t) \\ 1 & t \in \bigcup\limits_{k \in \mathbb{N}_{\text{even}}} [t_k + \Delta t, t_{k+1}) \end{cases} \quad (14)$$

where $\mathbb{N}_{\text{even}}$ and $\mathbb{N}_{\text{odd}}$ are used to denote the even and odd natural numbers, respectively. Based on the design in (14), χ and its first time derivative are bounded and continuous, and the second time derivative of χ is bounded. The transition period in (14) is defined as $\Delta t \triangleq (\pi)/(\omega)$ and can be made arbitrarily short through the choice of ω.

After substituting (13) into (11), the open-loop error dynamics can be expressed as

$$Jr = W - \bar{\Omega} V + \tau_d \quad (15)$$

where

$$\bar{\Omega} \triangleq \chi \Omega_i + (1 - \chi) \Omega_j, \quad i, j \in \mathbb{S}, i \neq j. \quad (16)$$

From (14), (16), and Assumption 1, $\bar{\Omega}$ is nonzero, positive, and bounded; the first two partial derivatives of $\bar{\Omega}$ with respect to q and $\dot{q}$ are bounded for a bounded argument; and the first two partial derivatives of $\bar{\Omega}$ with respect to time (via the time derivatives of φ_i and χ) are bounded. Furthermore, $\bar{\Omega} > \varepsilon > 0$, and thus, $\bar{\Omega}$ is invertible.

After multiplying (15) by $\bar{\Omega}^{-1}$, the open-loop error dynamics can be expressed as

$$J_\Omega r = W_\Omega - V + \tau_{d\Omega} \tag{17}$$

where

$$J_\Omega \triangleq \bar{\Omega}^{-1} J, W_\Omega \triangleq \bar{\Omega}^{-1} W, \ \tau_{d\Omega} \triangleq \bar{\Omega}^{-1} \tau_d.$$

To facilitate the subsequent stability analysis, the time derivative of (17) is expressed as

$$J_\Omega \dot{r} = -\frac{1}{2}\dot{J}_\Omega r + \tilde{N} + N_d - e_2 - \dot{V} \tag{18}$$

where $\tilde{N}, N_d \in \mathbb{R}$ denote the following auxiliary[1] terms

$$\begin{aligned}
\tilde{N} &\triangleq N - N_d, \\
N &\triangleq \dot{W}_\Omega + e_2 - \frac{1}{2}\dot{J}_\Omega r + \dot{\tau}_{d\Omega} \\
N_d &\triangleq \frac{1}{\bar{\Omega}_d} N_{d1} - \frac{\dot{\bar{\Omega}}_d}{(\bar{\Omega}_d)^2} N_{d2} \\
N_{d1} &\triangleq J\dddot{q}_d + \dot{M}_e(q_d) + \dot{M}_g(q_d) + \dot{M}_v(\dot{q}_d) + \dot{\tau}_d \\
N_{d2} &\triangleq J\ddot{q}_d + M_e(q_d) + M_g(q_d) + M_v(\dot{q}_d) + \tau_d \\
\bar{\Omega}_d &\triangleq \bar{\Omega}(q_d, \dot{q}_d, t).
\end{aligned}$$

Motivation for expressing the open-loop error system as in (18) is to separate the model into groups that are bounded by state-dependent bounds or by constants. Specifically, by applying the Mean Value Theorem ([44, Lemma 5]), $\tilde{N}$ can be upper-bounded by state-dependent terms as

$$|\tilde{N}| \leq \rho(\|z\|)\|z\| \tag{19}$$

where $\|\cdot\|$ denotes the standard 2-norm, $z \in \mathbb{R}^3$ is defined as

$$z \triangleq [e_1, \ e_2, \ r]^T \tag{20}$$

and $\rho : \mathbb{R} \to \mathbb{R}$ is a positive, strictly increasing function. The definition of the desired trajectory can be used to prove the upper bounds for N_d as

$$|N_d| \leq \zeta_{N_d}, \quad |\dot{N}_d| \leq \zeta_{\dot{N}_d} \tag{21}$$

where $\zeta_{N_d}, \ \zeta_{\dot{N}_d} \in \mathbb{R}$ are known, positive constants.

Remark 2: The bounds on N_d and $\dot{N}_d$ depend on the signal χ since $\dot{\chi}$ and $\ddot{\chi}$ appear through $\dot{\bar{\Omega}}$ and $\ddot{\bar{\Omega}}$. A sufficient condition for stability of the closed-loop error system will later be shown to depend on the bounds of N_d and $\dot{N}_d$. Therefore, a sufficient condition for stability of the closed-loop error system depends on the transition period Δt. However, the transition period can be made arbitrarily small by selecting control gains based on the desired length of the transition period.

Based on the open-loop error system in (18) and the subsequent stability analysis, a RISE-based (Robust Integral of the Sign of the Error) controller [45] is designed as

$$V \triangleq (k_s + 1)(e_2 - e_2(0)) + \nu \tag{22}$$

where ν is the generalized Filippov solution to

$$\dot{\nu} = (k_s + 1)\alpha_2 e_2 + \beta \operatorname{sgn}(e_2), \ \nu(0) = \nu_0 \tag{23}$$

where $k_s, \ \beta \in \mathbb{R}$ are positive, selectable control gains, ν_0 is a user-defined initial voltage, and $\operatorname{sgn}(\cdot)$ denotes the signum function.

Remark 3: In the subsequent experiments, the pulsewidth will be adjusted according to the control law in (22) and (23) rather than the voltage. During NMES, there are three stimulation parameters that affect the resulting torque: pulse amplitude (voltage amplitude or equivalently current amplitude), pulsewidth, and pulse frequency. Typically two of these three parameters are fixed while the final parameter is varied to evoke the desired muscle response. The uncertain model in (17) relating the stimulus input V to the evoked torque is equivalent regardless of which parameter is varied. Therefore, the stimulus input was referred to as a voltage in the control development and modeling sections to be consistent with the RISE-based controller that was developed for conventional stimulation in [40]. Meanwhile, the pulsewidth was varied during experiments in the present work since the utilized stimulator has a greater resolution on pulsewidth (20–500 μs in steps of 1 μs) than current amplitude (0–126 mA in steps of 2 mA).

After substituting (22) into (18) and using the definition of r in (9), the closed-loop dynamics can be written as

$$\begin{aligned}
J_\Omega \dot{r} = -\frac{1}{2}\dot{J}_\Omega r + \tilde{N} + N_d - e_2 \\
- (k_s + 1)r - \beta \operatorname{sgn}(e_2). \quad (24)
\end{aligned}$$

The closed-loop system in (24) yields semi-global asymptotic tracking of a desired knee-joint trajectory as described in the following theorem.

Theorem 1: The controller designed in (22) yields semi-global asymptotic tracking in the sense that

$$|e_1| \to 0 \ as \ t \to \infty$$

under any switching signal satisfying Property 1, provided the control gain k_s, introduced in (22) and (23), is selected sufficiently large according to the initial conditions, and the control gains α_1, α_2, and β introduced in (8), (9), and (23) are selected according to the following sufficient conditions:

$$\alpha_1 > \frac{1}{2}, \ \alpha_2 > 1 \tag{25}$$

$$\beta > \left(\zeta_{N_d} + \frac{1}{\alpha_2}\zeta_{\dot{N}_d}\right) \tag{26}$$

where ζ_{N_d}, and $\zeta_{\dot{N}_d}$ were introduced in (21).

Proof: See the Appendix. ■

[1]The terms $\tilde{N}$ and N_d are not available for use in the controller and are introduced only to facilitate the stability analysis. These terms are not used in the controller because they depend on the dynamics that contain parametric uncertainty (e.g., J, m, l, B_1, k_{e1}, η, τ_d, and $\dot{\tau}_d$ are uncertain). Moreover, $\tilde{N}$ contains r, which depends on angular acceleration measurements. Motivation to exclude r from the controller is that acceleration measurements contain high frequency measurement/numerical artifacts that can inject high frequency content in the controller.

IV. Experiments

Asynchronous and conventional stimulation were examined during dynamic contractions to better understand the NMES-induced fatigue characteristics of the stimulation protocols. For both asynchronous and conventional stimulation, the control algorithm in (22) and (23) was used to vary the pulsewidth in real time while the current amplitude and stimulation frequency remained constant.

A. Subjects

Four able-bodied individuals (male, aged 20–27) participated in the study. Prior to participation, written informed consent was obtained from all participants, as approved by the institutional review board at the University of Florida.

B. Apparatus

All testing was performed using an apparatus that consisted of the following.

1) A current-controlled 8-channel stimulator (RehaStim, Hasomed GmbH, operating in ScienceMode).
2) A data acquisition device (Quanser Q8-USB).
3) A personal computer running Matlab/Simulink.
4) A leg extension machine (shown previously in Fig. 2) that was modified to include sensors as well as boots to securely fasten the shank and foot.
5) Optical encoders to measure the leg angle (BEI Technologies).
6) Electrodes (Axelgaard Manufacturing Co., Ltd.)[2].

C. Stimulation Protocols

Two stimulation protocols were examined: 16 Hz asynchronous stimulation (A16) with four channels and 64 Hz conventional stimulation (C64) with a single channel. These two protocols were selected because A16 has a composite stimulation frequency equivalent to C64. Conventional stimulation consisted of a single stimulation channel with a pair of 3 in $\times$ 5 in Valutrode surface electrodes placed distally and proximally over the quadriceps femoris muscle group, while asynchronous stimulation consisted of four channels of stimulation utilizing four electrodes placed distally (1.5 in $\times$ 3.5 in Valutrode) and two electrodes placed proximally (2 in $\times$ 3.5 in Valutrode). For asynchronous stimulation, the electrical pulses were interleaved across the stimulation channels. In other words, asynchronous stimulation of 16 Hz with four channels resulted in a composite stimulation frequency of 64 Hz. The electrode configurations utilized for conventional and asynchronous stimulation are depicted in Fig. 4, and the method of interleaving the pulses across the stimulation channels was as previously depicted for asynchronous stimulation in Fig. 1.

D. Precautions

To prevent any layover effect of fatigue, each leg received only one stimulation protocol per day. On the first day of experiments, the two stimulation protocols (A16 and C64) were randomly divided between the individual's left and right legs.

[2]Surface electrodes for the study were provided compliments of Axelgaard Manufacturing Co., Ltd.

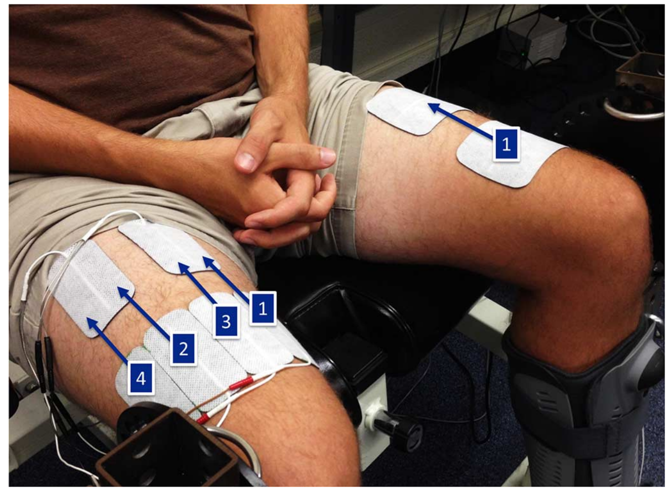

Fig. 4. Electrode configurations utilized for conventional and asynchronous stimulation. Pictured above is single-channel conventional stimulation on the individual's left leg and four-channel asynchronous stimulation on the individual's right leg. Conventional stimulation consists of one stimulation channel with one electrode placed proximally and one electrode placed distally. Asynchronous stimulation consists of four stimulation channels with two electrodes placed proximally and four electrodes placed distally. Stimulation channels 1 and 3 share the most medial and proximal electrode, while channels 2 and 4 share the most lateral and proximal electrode.

While a minimum of 24 h of rest was required before the individual completed the remaining protocol for each leg, additional rest was allowed if the individual reported symptoms of muscle fatigue.

E. Pretrial Tests

The control gains[3] were adjusted in pretrial tests to achieve trajectory tracking where the desired angular trajectory[4] of the knee joint was selected as a sinusoid ranging from 5° to 50° with a period of 2 s. The root mean square (rms) position tracking error was calculated in real time with a moving window of 2 s to assist the gain tuning process. After determining appropriate control gains in the pretrial tests, fatigue trials were subsequently conducted on the same day. Since there is a finite pulsewidth resolution for the stimulator (steps of 1 μs), the current amplitude must be selected small enough so that there is a sufficient range of pulsewidth values corresponding to the desired range of motion. However, the current amplitude must also be selected large enough so that the pulsewidth does not saturate. Furthermore, the muscle response to stimulation varies from person to person and asynchronous stimulation has been commonly reported to require less current amplitude to reach the same value of torque as conventional stimulation [23], [25], [46]. Therefore, the current amplitude was selected for each leg/protocol during the pretrial tests so that the resulting pulsewidth (calculated by the control algorithm) had sufficient range to elicit controlled limb movement without saturating.

[3]To ensure a fair comparison, efforts were made to utilize the same control gains for asynchronous and conventional stimulation. While this is not always possible due to general variability in the muscle response to stimulation, the control gains (other than the general scaling factor k_s) were the same for both asynchronous and conventional stimulation in five out of the eight legs tested, with minor gain variations in the remaining three legs.

[4]The desired trajectory was based on the comfortable range of motion.

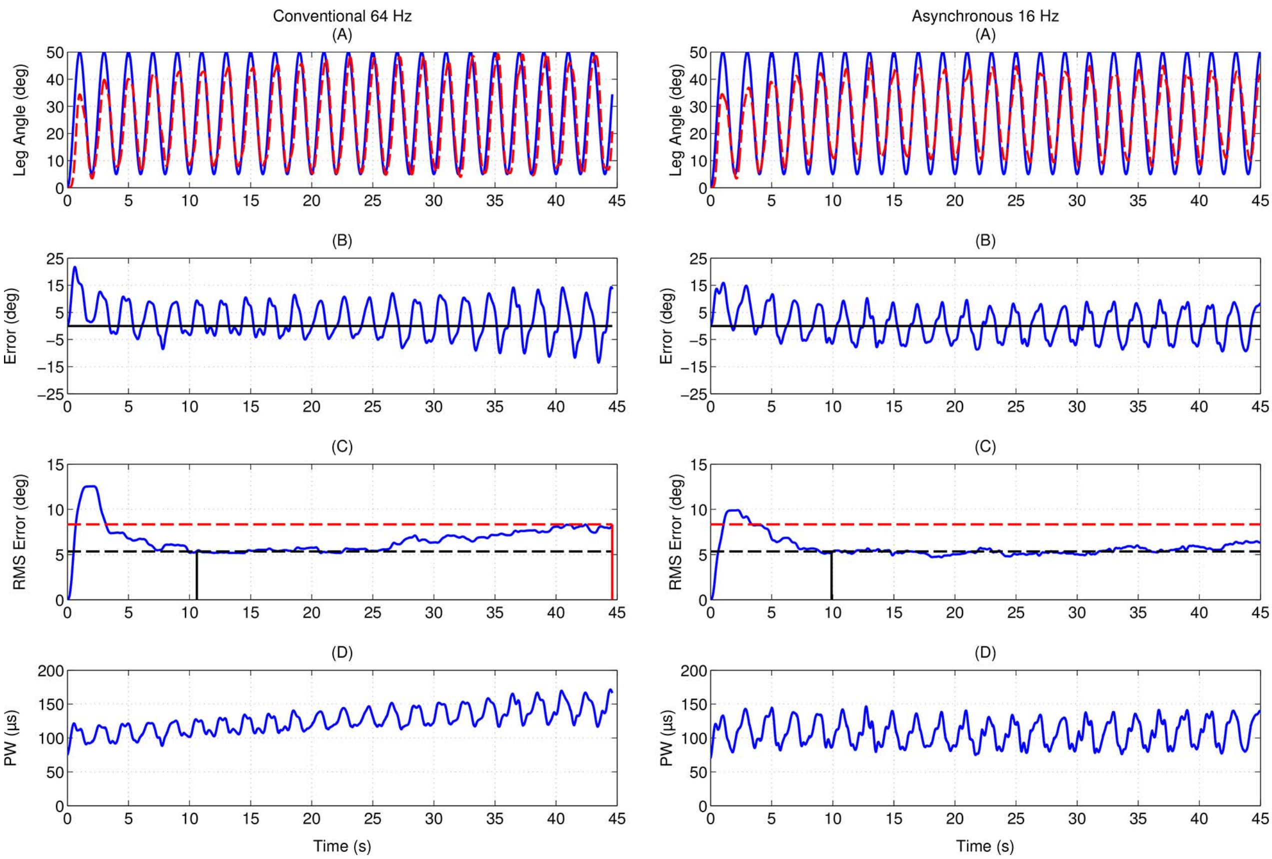

Fig. 5. Example tracking performance for conventional stimulation (left column) and asynchronous stimulation (right column) taken from the right leg of Subject D. Plot A depicts the desired (solid line) and actual (dashed line) leg angle. Plot B depicts the position tracking error. Plot C depicts the rms tracking error calculated over a moving 2-s window. The dashed lines in Plot C indicate the baseline error and the threshold that determines when to terminate stimulation (3° of rms error above the baseline measurement). Vertical solid lines correspond to the time that steady state tracking began and the time that the rms error increased by 3°. Note that the end time is not shown for asynchronous stimulation so that the two protocols can be visually compared over the same time scale. Plot D depicts the pulsewidth (i.e., the control input) that was calculated according to the developed control algorithm and delivered to the quadriceps femoris muscle group.

F. Fatigue Trials

Fatigue trials were conducted where the pulsewidth was adjusted according to the developed feedback control algorithm in (22) and (23) to compare each stimulation protocol in terms of its ability to maintain trajectory tracking. The baseline rms tracking error was calculated when the tracking error had reached steady state.[5] The successful run time (SRT) of each fatigue trial was then calculated as the elapsed time from the onset of steady state tracking to the time that the rms tracking error increased by 3° above the baseline measurement.

G. Statistical Analysis

The difference between the SRTs for asynchronous and conventional stimulation was calculated (i.e., paired data). A sign test was performed at a significance level of $\alpha = 0.05$ to test for statistically significant differences between the two protocols. Similarly, a sign test was used to test for statistically significant differences between the baseline rms errors. In addition to the sign test, a 95% confidence interval was constructed for the median difference between the SRTs of asynchronous and conventional stimulation to better quantify the relative performance of the two protocols.

V. Results

The SRTs for each fatigue trial are listed in Table I, and the corresponding baseline rms errors are listed in Table II. Asynchronous stimulation yielded a significantly longer SRT than conventional stimulation $(\mathrm{P}-\mathrm{Value} = 0.0078)$. Meanwhile, the baseline rms errors were not significantly different $(\mathrm{P}-\mathrm{Value} = 0.7266)$. The 95% confidence interval for the median difference between the SRTs of asynchronous and conventional stimulation was found to be (30.8, 67.3) seconds. The mean current amplitude was 65 and 85 mA for the asynchronous and conventional stimulation fatigue trials, respectively. Example fatigue trials comparing asynchronous and conventional stimulation are shown in Fig. 5.

For the left leg of Subject B, the electrodes for both asynchronous and conventional stimulation were moved farther towards the medial side of the leg. The electrode positions were different in this particular instance because the muscle consistently exhibited an "all-or-nothing" response to stimulation whenever an electrode was placed superficial to the vastus lateralis. The necessary shifting of electrodes for the left leg of Subject B may explain why this trial exhibited the shortest

[5]The onset of steady state tracking is defined as the point at which the rms error begins to flatten (no longer decreasing from the large initial error). Steady state tracking occurred approximately 10 s after starting the trial, on average.

TABLE I
SUCCESSFUL RUN TIME (IN SECONDS)

Subject-Leg	C64	A16	Difference
A - Left	53.4	85.1	31.7
A - Right	37.3	76.3	38.9
B - Left	26.2	45.4	19.2
B - Right	21.3	64.7	43.3
C - Left	27.1	93.6	66.4
C - Right	20.9	66.6	45.7
D - Left	33.7	94.8	61.1
D - Right	34.0	113.4	79.4
25th Percentile	**22.6**	**65.1**	**33.5**
Median	**30.4**	**80.7**	**44.5***
75th Percentile	**36.5**	**94.5**	**65.1**

∗ *SRT of asynchronous stimulation is significantly longer than that of conventional stimulation*

TABLE II
BASELINE RMS ERROR (DEGREES)

Subject-Leg	C64	A16	Difference
A - Left	5.16	5.03	-0.13
A - Right	4.88	4.69	-0.19
B - Left	5.64	4.52	-1.12
B - Right	4.37	5.19	0.82
C - Left	4.78	4.71	-0.07
C - Right	5.69	5.91	0.22
D - Left	4.82	4.88	0.07
D - Right	5.34	5.34	-0.00
25th Percentile	**4.79**	**4.69**	**-0.18**
Median	**5.02**	**4.96**	**-0.04**
75th Percentile	**5.57**	**5.30**	**0.18**

SRT of all asynchronous stimulation trials (see Table I) since crowding the electrodes to the medial side may have caused overlap in the muscle activation. In other words, some muscle fibers may have been activated by more than one electrode in this particular trial thereby reducing the fatigue benefits of asynchronous stimulation.

VI. DISCUSSION

Asynchronous stimulation has been previously shown to have significant advantages over conventional stimulation [21]–[34] in terms of reduced fatigue. However, studies comparing asynchronous to conventional stimulation have primarily focused on isometric contractions with fixed stimulation parameters [21]–[25], [28]–[32], [34], due to the fact that it is easier to control for variation in the data. Sequential stimulation has also been shown to be advantageous over conventional stimulation as a method to reduce fatigue in isometric contractions [36], [37]. However, one study [36] found that a shorter on-time (i.e., the time to keep one stimulation channel activated before switching to the next channel) resulted in less fatigue, motivating the use of asynchronous stimulation over sequential stimulation. Furthermore, depending on the application, sequential stimulation may not be viable. For example, due to the segregation of motor units and the fact that sequential stimulation switches between stimulation channels less frequently, the torque required to accomplish a task may be greater than the torque that a single stimulation channel can maintain. Meanwhile, for asynchronous stimulation, even if one stimulation channel elicits a particularly weak response, the more frequent switching provides an averaging effect such that a larger torque can be maintained. In the present study, the developed control method is theoretically applicable to both sequential stimulation and asynchronous stimulation. However, in preliminary tests, asynchronous stimulation was reported to be more comfortable than sequential stimulation. Therefore, the experimental work of the present study focused on asynchronous stimulation.

While experiments reported in literature have primarily been conducted with isometric contractions, a few studies have examined contractions yielding limb motion. Asynchronous stimulation [26] and sequential stimulation [35] were shown to reduce fatigue during FES cycling. Asynchronous stimulation has also been shown to be beneficial for isotonic gripping [27]. However, in the three aforementioned studies, the stimulus was delivered in an open-loop manner. Normann *et al.* used asynchronous stimulation to reduce fatigue during standing in cats [47]. While stimulation was also delivered in an open-loop manner, the authors stated that feedback information would be required if the method were to be used for a clinical neuroprosthesis. Similarly, Lau *et al.* studied standing in cats with both asynchronous and conventional stimulation [33]. As expected, the authors found that asynchronous resulted in less fatigue than conventional stimulation. The authors also compared open-loop and closed-loop control and found that the duration of standing achieved with closed-loop control was longer than that for open-loop control. However, the closed-loop controller implemented was a logic-based if-then-else algorithm. More recently, Frankel *et al.* implemented an iterative learning controller for isometric force control in cats; however, no modeling or stability analysis was included and the results were not compared with conventional stimulation [48].

In the current result, a controller that enables limb trajectory tracking was designed based on a constructive stability analysis (see the Appendix) that included the nonlinear, uncertain muscle/limb dynamics, and the controller performance was experimentally demonstrated in both legs of four able-bodied individuals. The experiments indicate that asynchronous stimulation can successfully extend the duration of successful limb tracking compared to conventional stimulation in man. This result is promising for various rehabilitative treatments since a longer SRT means a larger dose of rehabilitative stimulation can be delivered before the onset of fatigue. The result is also promising for the development of neuroprostheses that may require the use of feedback control since asynchronous stimulation could slow the rate of fatigue, and thereby extend the duration that a neuroprosthesis enables functional movements or activities of daily living. Although experiments were conducted only in able-bodied individuals in the present study, asynchronous stimulation has been previously shown to slow the rate of fatigue (without feedback control) in individuals post-stroke [27] and in individuals with spinal cord injury [23]–[25], [34]. Therefore, it is expected that feedback control with asynchronous stimulation would result in longer durations of successful limb tracking than conventional stimulation in patient populations, similar to the able-bodied population of the present study. Nonetheless, experimental validation is still required to know the extent that the SRT can be prolonged during feedback control for individuals with spinal cord injury and other neurological disorders. Furthermore, experimental validation is still required to investigate the clinical significance of longer SRTs (and thus larger rehabilitative doses) in disease/injury specific populations.

While the present results are promising, additional opportunities exist for closed-loop asynchronous stimulation. For example, since the muscle response to stimulation is different for each stimulation channel, it may be beneficial to develop a controller where the control gains can be selected independently for each channel. Independent gains may be particularly important if multiple heads of a large muscle are stimulated since different heads could have different recruitment and fatigue properties. Additionally, low-frequency asynchronous stimulation can lead to force ripple [46]. While the 16 Hz asynchronous stimulation protocol utilized in the present study resulted in smooth traces (see Fig. 5) and has been previously shown to induce equivalent ripple to volitional contractions [46], future efforts could focus on reducing force ripple for low-frequency asynchronous stimulation either through independent gains or adaptive control laws. Adaptive controllers may also prove to be beneficial for asynchronous stimulation since they typically require less control effort and result in better tracking performance than robust controllers in practice. Future efforts could also focus on developing and/or implementing asynchronous stimulation with closed-loop control for other activities such as standing or cycling.

Appendix A
Stability Analysis

Proof: Let $y \in D \subset \mathbb{R}^{3+1}$, defined as

$$y \triangleq [z^T,\ \sqrt{P}]^T \tag{27}$$

where z was defined in (20) and $P \in \mathbb{R}$ is the Filippov solution to

$$\begin{aligned}\dot{P} &= -r[N_d - \beta \operatorname{sgn}(e_2)]\\ P(e_2(0), 0) &= -e_2(0)N_d(0) + |e_2(0)|\beta.\end{aligned} \tag{28}$$

Provided the gain condition for β in (26) is satisfied, P is guaranteed to satisfy $P \geq 0$ ([45, Lemma 1]).

Let $V_L : D \to \mathbb{R}$ be a continuously differentiable function, defined as

$$V_L \triangleq e_1^2 + \frac{1}{2}e_2^2 + \frac{1}{2}J_\Omega r^2 + P \tag{29}$$

which satisfies the following inequalities:

$$U_1 \leq V_L \leq U_2 \tag{30}$$

where $U_1, U_2 \in \mathbb{R}$ are continuous, positive definite functions defined as $U_1 \triangleq \lambda_1\|y\|^2$, $U_2 \triangleq \lambda_2\|y\|^2$, where y was defined in (27) and $\lambda_1, \lambda_2 \in \mathbb{R}$ are positive constants.

The time derivative of (29) exists almost everywhere (a.e.)[6], i.e., for almost all $t \in [0, \infty)$, and $\dot{V}_L \overset{a.e.}{\in} \dot{\tilde{V}}_L$ where

$$\dot{\tilde{V}}_L \triangleq \bigcap_{\xi \in \partial V_L} \xi^T K\left[\dot{e}_1, \dot{e}_2, \dot{r}, \frac{1}{2}P^{-\frac{1}{2}}\dot{P}, 1\right]^T \tag{31}$$

where $K[\cdot]$ is defined in [49], and ∂V_L is the generalized gradient of V_L. Since V_L is continuously differentiable with respect to y, (31) can be rewritten as

$$\dot{\tilde{V}}_L \subset \nabla V_L^T K\left[\dot{e}_1,\ \dot{e}_2, \dot{r}, \frac{1}{2}P^{-\frac{1}{2}}\dot{P}, 1\right]^T \tag{32}$$

where

$$\nabla V_L \triangleq \left[2e_1, e_2, rJ_\Omega, 2P^{\frac{1}{2}}, \frac{1}{2}\dot{J}_\Omega r^2\right]^T.$$

Substituting (7)–(9) and (24) into (32) yields

$$\begin{aligned}\dot{\tilde{V}}_L \subset\ & 2e_1(e_2 - \alpha_1 e_1) + e_2(r - \alpha_2 e_2) + \frac{1}{2}r\dot{J}_\Omega r\\ &+ r\left(-\frac{1}{2}\dot{J}_\Omega r + N_d - e_2\right) + K\left[\dot{P}\right]\\ &+ r\left(\tilde{N} - (k_s+1)r - \beta K[\operatorname{sgn}](e_2)\right)\end{aligned} \tag{33}$$

where $K[\operatorname{sgn}](e_2) = 1$ if $e_2 > 0$, $[-1, 1]$ if $e_2 = 0$, and -1 if $e_2 < 0$. After substituting $\dot{P}$ from (28) and canceling common terms, (33) can be rewritten and upper-bounded as

$$\begin{aligned}\dot{V}_L \overset{a.e.}{\leq}\ & -2\alpha_1 e_1^2 - \alpha_2 e_2^2 + 2|e_1||e_2|\\ &+ r\tilde{N} - (k_s+1)r^2\end{aligned} \tag{34}$$

where the set in (33) reduces to the scalar inequality in (34) since the right hand side is continuous almost everywhere, i.e., the right-hand side is continuous except for the Lebesgue negligible set of times when

$$r\beta K[\operatorname{sgn}](e_2) - r\beta K[\operatorname{sgn}](e_2) \neq \{0\}.$$

After utilizing Young's Inequality and (19), the inequality in (34) can be further upper-bounded as

$$\begin{aligned}\dot{V}_L \overset{a.e.}{\leq}\ & -(2\alpha_1 - 1)e_1^2 - (\alpha_2 - 1)e_2^2\\ &- (k_s+1)r^2 + \rho(\|z\|)\|z\||r|.\end{aligned} \tag{35}$$

After completing the square, (35) can be expressed as

$$\begin{aligned}\dot{V}_L &\overset{a.e.}{\leq} -\left(\lambda - \frac{\rho^2(\|z\|)}{4k_s}\right)\|z\|^2\\ &\overset{a.e.}{\leq} -U_3 \triangleq -c\|z\|^2, \forall y \in D\end{aligned} \tag{36}$$

where $\lambda \triangleq \min\{2\alpha_1 - 1, \alpha_2 - 1, 1\}$, $c \in \mathbb{R}$ is a positive constant, and D is defined as

$$D \triangleq \{y \in \mathbb{R}^{3+1} \mid \rho(\|y\|) < \sqrt{4\lambda k_s}\}$$

[6]The time derivative of the Lyapunov function has a discontinuous right-hand side (due to $\dot{V}$ and $\dot{P}$), causing the time derivative of the Lyapunov function to exist almost everywhere and motivating the nonsmooth analysis.

where ρ was introduced in (19). From the inequalities in (30) and (36), $V_L \in \mathcal{L}_\infty$, and hence, $e_1, e_2, r \in \mathcal{L}_\infty$. The remaining signals in the closed-loop dynamics can be proven to be bounded. Let $D_z \subset D$ be defined as

$$D_z \triangleq \left\{ y \in D \mid \rho \left(\sqrt{\frac{\lambda_2}{\lambda_1}} \|y\| \right) < \sqrt{4\lambda k_s} \right\}. \tag{37}$$

From (36), ([50, Corollary 1]) can be invoked to show that $c\|z\|^2 \to 0$ as $t \to \infty$, $\forall y(0) \in D_z$. Based on the definition of z, $e_1 \to 0 \; as \; t \to \infty$, $\forall\, y(0) \in D_z$. Note that the region of attraction in (37) can be expanded arbitrarily by increasing k_s. Provided that the gain conditions in (25) and (26) are satisfied, the result of the stability analysis is independent of the designed switching signals σ satisfying Property 1, so that the asymptotic tracking result is satisfied where the only restriction on the switching signal is that there be an arbitrarily short transition period during which two stimulation channels are simultaneously activated. ■

References

[1] T. Mohr *et al.*, "Increased bone mineral density after prolonged electrically induced cycle training of paralyzed limbs in spinal cord injured man," *Calcif. Tissue Int.*, vol. 61, no. 1, pp. 22–25, 1997.

[2] M. Bélanger, R. B. Stein, G. D. Wheeler, T. Gordon, and B. Leduc, "Electrical stimulation: Can it increase muscle strength and reverse osteopenia in spinal cord injured individuals?," *Arch. Phys. Med. Rehabil.*, vol. 81, no. 8, pp. 1090–1098, 2000.

[3] L. Griffin *et al.*, "Functional electrical stimulation cycling improves body composition, metabolic and neural factors in persons with spinal cord injury," *J. Electromyogr. Kinesiol.*, vol. 19, no. 4, pp. 614–622, 2009.

[4] M. M. Rodgers *et al.*, "Musculoskeletal responses of spinal cord injured individuals to functional neuromuscular stimulation-induced knee extension exercise training," *J. Rehabil. Res. Dev.*, vol. 28, no. 4, pp. 19–26, 1991.

[5] S. P. Hooker *et al.*, "Physiologic effects of electrical stimulation leg cycle exercise training in spinal cord injured persons," *Arch. Phys. Med. Rehabil.*, vol. 73, no. 5, pp. 470–476, 1992.

[6] E. Ambrosini, S. Ferrante, G. Ferrigno, F. Molteni, and A. Pedrocchi, "Cycling induced by electrical stimulation improves muscle activation and symmetry during pedaling in hemiparetic patients," *IEEE Trans. Neural Syst. Rehabil. Eng.*, vol. 20, no. 3, pp. 320–330, May 2012.

[7] S. K. Sabut, C. Sikdar, R. Mondal, R. Kumar, and M. Mahadevappa, "Restoration of gait and motor recovery by functional electrical stimulation therapy in persons with stroke," *Disabil. Rehabil.*, vol. 32, no. 19, pp. 1594–1603, 2010.

[8] B. M. Doucet and L. Griffin, "Maximal versus submaximal intensity stimulation with variable patterns," *Muscle Nerve*, vol. 37, no. 6, pp. 770–777, 2008.

[9] M. B. Kebaetse and S. A. Binder-Macleod, "Strategies that improve human skeletal muscle performance during repetitive, non-isometric contractions," *Pflügers Arch.*, vol. 448, no. 5, pp. 525–532, Aug. 2004.

[10] B. Bigland-Ritchie, I. Zijdewind, and C. K. Thomas, "Muscle fatigue induced by stimulation with and without doublets," *Muscle Nerve*, vol. 23, no. 9, pp. 1348–1355, Sep. 2000.

[11] R. J. Downey *et al.*, "A novel modulation strategy to increase stimulation duration in neuromuscular electrical stimulation," *Muscle Nerve*, vol. 44, no. 3, pp. 382–387, Sept. 2011.

[12] G. M. Graham, T. A. Thrasher, and M. R. Popovic, "The effect of random modulation of functional electrical stimulation parameters on muscle fatigue," *IEEE Trans. Neural Syst. Rehabil. Eng.*, vol. 14, no. 1, pp. 38–45, Mar. 2006.

[13] E. Henneman, G. Somjen, and D. O. Carpenter, "Functional significance of cell size in spinal motoneurons," *J. Neurophysiol.*, vol. 28, pp. 560–580, 1965.

[14] R. J. Kubiak, K. M. Whitman, and R. M. Johnston, "Changes in quadriceps femoris muscle strength using isometric exercise versus electrical stimulation," *J. Orthop. Sports Phys. Ther.*, vol. 8, no. 11, pp. 537–541, 1987.

[15] D. R. Sinacore, A. Delitto, D. S. King, and S. J. Rose, "Type II fiber activation with electrical stimulation: A preliminary report," *Phys. Ther.*, vol. 70, no. 7, pp. 416–422, July 1990.

[16] C. M. Gregory and C. S. Bickel, "Recruitment patterns in human skeletal muscle during electrical stimulation," *Phys. Ther.*, vol. 85, no. 4, pp. 358–364, 2005.

[17] C. S. Bickel, C. M. Gregory, and J. C. Dean, "Motor unit recruitment during neuromuscular electrical stimulation: A critical appraisal," *Eur. J. Appl. Physiol.*, vol. 111, no. 10, pp. 2399–2407, 2011.

[18] C. M. Gregory, W. E. Dixon, and C. S. Bickel, "Impact of varying pulse frequency and duration on muscle torque production and fatigue," *Muscle Nerve*, vol. 35, no. 4, pp. 504–509, Apr. 2007.

[19] S. A. Binder-Macleod, E. E. Halden, and K. A. Jungles, "Effects of stimulation intensity on the physiological responses of human motor units," *Med. Sci. Sports. Exerc.*, vol. 27, no. 4, pp. 556–565, Apr. 1995.

[20] D. A. Jones, B. Bigland-Ritchie, and R. H. T. Edwards, "Excitation frequency and muscle fatigue: Mechanical responses during voluntary and stimulated contractions," *Exp. Neurol.*, vol. 64, no. 2, pp. 401–413, May 1979.

[21] D. McDonnall, G. A. Clark, and R. A. Normann, "Interleaved, multisite electrical stimulation of cat sciatic nerve produces fatigue-resistant, ripple-free motor responses," *IEEE Trans. Neural Syst. Rehabil. Eng.*, vol. 12, no. 2, pp. 208–215, Jun. 2004.

[22] A. C. Hughes, L. Guo, and S. P. DeWeerth, "Interleaved multichannel epimysial stimulation for eliciting smooth contraction of muscle with reduced fatigue," in *Proc. Annu. Int. Conf. IEEE Eng. Med. Biol. Soc.*, Sep. 2010, pp. 6226–6229.

[23] L. Z. Popović and N. M. Malešević, "Muscle fatigue of quadriceps in paraplegics: Comparison between single vs. multi-pad electrode surface stimulation," in *Proc. Annu. Int. Conf. IEEE Eng. Med. Biol. Soc.*, Sep. 2009, pp. 6785–6788.

[24] N. M. Malešević, L. Z. Popović, L. Schwirtlich, and D. B. Popović, "Distributed low-frequency functional electrical stimulation delays muscle fatigue compared to conventional stimulation," *Muscle Nerve*, vol. 42, no. 4, pp. 556–562, 2010.

[25] R. Nguyen, K. Masani, S. Micera, M. Morari, and M. R. Popovic, "Spatially distributed sequential stimulation reduces fatigue in paralyzed triceps surae muscles: A case study," *Artif. Organs*, vol. 35, no. 12, pp. 1174–1180, 2011.

[26] R. J. Downey *et al.*, "Asynchronous stimulation with an electrode array reduces muscle fatigue during FES cycling," in *Proc. Int. Func. Elect. Stimul. Soc.*, Banff, Canada, Sep. 2012, pp. 154–157.

[27] L. Z. P. Maneski, N. M. Malešević, A. M. Savić, T. Keller, and D. B. Popović, "Surface-distributed low-frequency asynchronous stimulation delays fatigue of stimulated muscles," *Muscle Nerve*, vol. 48, no. 6, pp. 930–937, 2013.

[28] M. Thomsen and P. H. Veltink, "Influence of synchronous and sequential stimulation on muscle fatigue," *Med. Biol. Eng. Comput.*, vol. 35, no. 3, pp. 186–192, 1997.

[29] D. G. Sayenko, R. Nguyen, M. R. Popovic, and K. Masani, "Reducing muscle fatigue during transcutaneous neuromuscular electrical stimulation by spatially and sequentially distributing electrical stimulation sources," *Eur. J. Appl. Physiol.*, vol. 114, no. 4, pp. 793–804, 2014.

[30] V. K. Mushahwar and K. W. Horch, "Proposed specifications for a lumbar spinal cord electrode array for control of lower extremities in paraplegia," *IEEE Trans. Rehabil. Eng.*, vol. 5, no. 3, pp. 237–243, Sep. 1997.

[31] A. K. Wise, D. L. Morgan, J. E. Gregory, and U. Proske, "Fatigue in mammalian skeletal muscle stimulated under computer control," *J. Appl. Physiol.*, vol. 90, no. 1, pp. 189–197, 2001.

[32] K. Yoshida and K. Horch, "Reduced fatigue in electrically stimulated muscle using dual channel intrafascicular electrodes with interleaved stimulation," *Ann. Biomed. Eng.*, vol. 21, no. 6, pp. 709–714, 1993.

[33] B. Lau, L. Guevremont, and V. K. Mushahwar, "Strategies for generating prolonged functional standing using intramuscular stimulation or intraspinal microstimulation," *IEEE Trans. Neural Syst. Rehabil. Eng.*, vol. 15, no. 2, pp. 273–285, Jun. 2007.

[34] R. J. Downey, M. J. Bellman, H. Kawai, C. M. Gregory, and W. E. Dixon, "Comparing the induced muscle fatigue between asynchronous and synchronous electrical stimulation in able-bodied and spinal cord injured populations," *IEEE Trans. Neural Syst. Rehabil. Eng.*, to be published.

[35] M. J. Decker, L. Griffin, L. D. Abraham, and L. Brandt, "Alternating stimulation of synergistic muscles during functional electrical stimulation cycling improves endurance in persons with spinal cord injury," *J. Electromyogr. Kinesiol.*, vol. 20, no. 6, pp. 1163–1169, 2010.

[36] M. Pournezam, B. J. Andrews, R. H. Baxendale, G. F. Phillips, and J. P. Paul, “Reduction of muscle fatigue in man by cyclical stimulation,” *J. Biomed. Eng.*, vol. 10, no. 2, pp. 196–200, 1988.

[37] E. D. Zonnevijlle *et al.*, “Sequential segmental neuromuscular stimulation: An effective approach to enhance fatigue resistance,” *Plast. Reconstr. Surg.*, vol. 105, no. 2, pp. 667–673, 2000.

[38] R. W. Stremel and E. D. Zonnevijlle, “Re-animation of muscle flaps for improved function in dynamic myoplasty,” *Microsurgery*, vol. 21, no. 6, pp. 281–286, 2001.

[39] R. J. Downey, T.-H. Cheng, and W. E. Dixon, “Tracking control of a human limb during asynchronous neuromuscular electrical stimulation,” in *Proc. IEEE Conf. Decis. Control*, Florence, IT, Dec. 2013, pp. 139–144.

[40] N. Sharma, K. Stegath, C. M. Gregory, and W. E. Dixon, “Nonlinear neuromuscular electrical stimulation tracking control of a human limb,” *IEEE Trans. Neural Syst. Rehabil. Eng.*, vol. 17, no. 6, pp. 576–584, Jun. 2009.

[41] J. L. Krevolin, M. G. Pandy, and J. C. Pearce, “Moment arm of the patellar tendon in the human knee,” *J. Biomech.*, vol. 37, no. 5, pp. 785–788, 2004.

[42] T. Watanabe, R. Futami, N. Hoshimiya, and Y. Handa, “An approach to a muscle model with a stimulus frequency-force relationship for FES applications,” *IEEE Trans. Rehabil. Eng.*, vol. 7, no. 1, pp. 12–18, Mar. 1999.

[43] E. P. Widmaier, H. Raff, and K. T. Strang, *A.J. Vander, J.H. Sherman, and D.S. Luciano's Human Physiology: The Mechanisms of Body Function*, 9th ed. New York: McGraw-Hill, 2004.

[44] R. Kamalapurkar, J. A. Rosenfeld, J. Klotz, R. J. Downey, and W. E. Dixon, “(2014) Supporting lemmas for RISE-based control methods,” arXiv:1306.3432v3.

[45] B. Xian, D. M. Dawson, M. S. de Queiroz, and J. Chen, “A continuous asymptotic tracking control strategy for uncertain nonlinear systems,” *IEEE Trans. Autom. Control*, vol. 49, no. 7, pp. 1206–1211, Jul. 2004.

[46] R. J. Downey, M. Tate, H. Kawai, and W. E. Dixon, “Comparing the force ripple during asynchronous and conventional stimulation,” *Muscle Nerve*, vol. 50, no. 4, pp. 549–555, Oct. 2014.

[47] R. A. Normann *et al.*, “Coordinated, multi-joint, fatigue-resistant feline stance produced with intrafascicular hind limb nerve stimulation,” *J. Neural Eng.*, vol. 9, no. 2, pp. 1–13, 2012.

[48] M. A. Frankel *et al.*, “Multiple-input single-output closed-loop isometric force control using asynchronous intrafascicular multi-electrode stimulation,” *IEEE Trans. Neural Syst. Rehabil. Eng.*, vol. 19, no. 3, pp. 325–332, Jun. 2011.

[49] B. E. Paden and S. S. Sastry, “A calculus for computing Filippov's differential inclusion with application to the variable structure control of robot manipulators,” *IEEE Trans. Circuits Syst.*, vol. 34, no. 1, pp. 73–82, Jan. 1987.

[50] N. Fischer, R. Kamalapurkar, and W. E. Dixon, “LaSalle-Yoshizawa corollaries for nonsmooth systems,” *IEEE Trans. Autom. Control*, vol. 58, no. 9, pp. 2333–2338, Sep. 2013.

Ryan J. Downey received the B.S. degree in mechanical engineering from the University of Florida, Gainesville, FL, USA, in 2010, where he participated in a research experiences for undergraduates program (REU). He subsequently joined the Nonlinear Controls and Robotics group in 2010 to pursue his doctoral research. In 2011, he was accepted to an international exchange program (ATLANTIS CRISP) and received the M.S. degree in biomedical engineering from Politecnico di Milano, Milan, Italy, in 2012. Upon returning to the U.S., he received the M.S. degree in biomedical engineering from the University of Florida in 2012 as well as the M.S. and Ph.D. degrees in mechanical engineering in 2014 and 2015, respectively.

His research focuses on functional electrical stimulation and Lyapunov-based nonlinear control.

His work has been recognized by the 2015 American Automatic Control Council (AACC) O. Hugo Schuck (Best Paper) Award.

Teng-Hu Cheng received the B.S. and M.S. degrees in mechanical engineering from National Taiwan University, Taiwan, in 2007 and 2009, respectively. He joined the Nonlinear Controls and Robotics group at the University of Florida, Gainesville, FL, USA, as a doctoral student under the advisement of Dr. W. Dixon in August 2011.

During the summers of 2013 and 2014, he was a research intern with the Air Force Research Laboratory (AFRL), Eglin AFB and University of Florida REEF, aiding in designing cooperative control for networked systems with time-varying network topologies and developing event-driven control for networked systems. His research interests include networked system control, switched control, event-driven control, and nonlinear control.

His work has been recognized by the 2015 American Automatic Control Council (AACC) O. Hugo Schuck (Best Paper) Award.

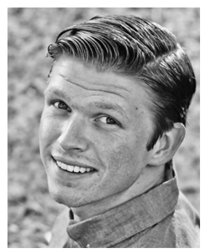

Matthew J. Bellman received the B.S. and M.S. (*magna cum laude*) degrees in mechanical engineering with a minor in biomechanics from the University of Florida, Gainesville, FL, USA. He is currently pursuing the Ph.D. degree in mechanical engineering as a National Defense Science and Engineering (NDSEG) Fellow, with a continued focus on the theoretical development of robust, adaptive control systems for applications involving functional electrical stimulation, specifically those involving rehabilitation and mobility of the lower extremities.

He has been a member of the Nonlinear Controls and Robotics group since May 2009.

His work has been recognized by the 2015 American Automatic Control Council (AACC) O. Hugo Schuck (Best Paper) Award.

Warren E. Dixon is a Professor in the Department of Mechanical and Aerospace Engineering at the University of Florida, Gainesville, FL, USA. His main research interests are the development and application of Lyapunov-based control techniques for uncertain nonlinear systems. He has published over 300 refereed papers and several books in this area. He has formerly served as an Associate Editor for several journals, and is currently an Associate Editor for *Automatica* and the *International Journal of Robust and Nonlinear Control*.

Dr. Dixon currently serves as a member of the U.S. Air Force Science Advisory Board and as the Director of Operations for the Executive Committee of the IEEE CSS Board of Governors. His work has been recognized by the 2013 Fred Ellersick Award for Best Overall MILCOM Paper, 2012–2013 University of Florida College of Engineering Doctoral Dissertation Mentoring Award, 2011 American Society of Mechanical Engineers (ASME) Dynamics Systems and Control Division Outstanding Young Investigator Award, 2009 and 2015 American Automatic Control Council (AACC) O. Hugo Schuck (Best Paper) Award, 2006 IEEE Robotics and Automation Society (RAS) Early Academic Career Award, an NSF CAREER Award (2006–2011), 2004 DOE Outstanding Mentor Award, and the 2001 ORNL Early Career Award for Engineering Achievement.